Cascade models for magnetohydrodynamic turbulence

D. Biskamp
Max-Planck-Institut für Plasmaphysik–EURATOM Association, D-85740 Garching, Germany
(Received 6 April 1994)

The complex cascade model by Gloaguen *et al.* [Physica D **17**, 154 (1985)] for magnetohydrodynamic turbulence is studied. In the first part the Alfvén effect is neglected. Stationary solutions are discussed. For purely kinetic turbulence a phenomenon, coherent structures in k spaces, is observed. For general magnetohydrodynamic turbulence, energy spectra are, in general, close to $k^{-5/3}$, and inertial-range statistics, in particular structure functions, are similar to those observed in hydrodynamic (fluid) turbulence. In the second part the Alfvén effect is included. For the simplest case of a constant large-scale field B_0, energy spectra are $k^{-1.25}$, flatter than the expected Iroshnikov-Kraichnan law $k^{-3/2}$, and the inertial-range statistics are exactly Gaussian. Hence, the model has to be refined. Assuming B_0 to be the actual fluctuating field, intermittency is reintroduced, and the spectrum is close to $k^{-3/2}$, though it tends to become flatter for high k, such that a uniformly valid inertial-range power-law spectrum may not exist.

PACS number(s): 47.27.Gs, 05.45.+b, 47.65.+a

I. INTRODUCTION

Turbulence in magnetized electrically conducting fluids occurs under rather general conditions in astrophysical as well as laboratory systems. Though the basic nonlinearities of the magnetohydrodynamic (MHD) equations are similar to those in Navier-Stokes theory, MHD turbulence exhibits a considerably richer and more complex behavior [1], which is primarily due to the presence of two solenoidal dynamical quantities, the velocity $\mathbf{v}$ and the magnetic field $\mathbf{B}$, following the equations

$$\partial_t \mathbf{v}+\mathbf{v}\cdot\nabla\mathbf{v}-\mathbf{B}\cdot\nabla\mathbf{B}=-\nabla p_t+\nu\nabla^2\mathbf{v}\ , \tag{1}$$

$$\partial_t \mathbf{B}+\mathbf{v}\cdot\nabla\mathbf{B}-\mathbf{B}\cdot\nabla\mathbf{v}=\eta\nabla^2\mathbf{B}\ , \tag{2}$$

$$\nabla\cdot\mathbf{v}=\nabla\cdot\mathbf{B}=0\ . \tag{3}$$

Here we have used the conventional normalizations: $x\to x/L$, $t\to tv_A/L$, $v\to v/v_A$, $\rho\to 1$, where $v_A=B_0/\sqrt{4\pi\rho}$ is the Alfvén speed corresponding to a typical magnetic intensity B_0 and L is a characteristic global scale length.

The total pressure $p_t=p+B^2/2$ is a functional of $\mathbf{v}$ and $\mathbf{B}$ owing to the incompressibility condition (3). The MHD equations can be written in a more symmetric form by introducing the Elsässer variables $\mathbf{P}=\mathbf{v}+\mathbf{B}$, $\mathbf{Q}=\mathbf{v}-\mathbf{B}$:

$$\partial_t \mathbf{P}+\mathbf{Q}\cdot\nabla\mathbf{P}=-\nabla p_t+\nu_+\nabla^2\mathbf{P}+\nu_-\nabla^2\mathbf{Q}\ , \tag{4}$$

$$\partial_t \mathbf{Q}+\mathbf{P}\cdot\nabla\mathbf{Q}=-\nabla p_t+\nu_+\nabla^2\mathbf{Q}+\nu_-\nabla^2\mathbf{P}\ , \tag{5}$$

$$\nu_\pm=(\nu\pm\eta)/2\ .$$

There are three quadratic ideal invariants

$$E=E^V+E^M=\tfrac{1}{2}\int(v^2+B^2)d\tau\ , \tag{6}$$

$$K=\tfrac{1}{2}\int\mathbf{v}\cdot\mathbf{B}\,d\tau\ , \tag{7}$$

$$H=\tfrac{1}{2}\int\mathbf{A}\cdot\mathbf{B}\,d\tau,\quad \nabla\times\mathbf{A}=\mathbf{B}\ , \tag{8}$$

or in two dimensions (2D)

$$H=\tfrac{1}{2}\int\psi^2 d\tau\ ,$$

the total energy E, the cross-helicity K, and the magnetic helicity H, or in 2D the mean square magnetic potential H^ψ. The corresponding spectral quantities E_k, K_k, H_k, or H_k^ψ follow detailed balance relations, which imply that once injected in some region of k space around some wave number k_0 these quantities propagate either to higher k corresponding to a direct spectral cascade or to lower k corresponding to an inverse cascade. While the mixed kinetic-magnetic quantities E_k and K_k exhibit direct cascades, the pure magnetic ones, H_k^A or H_k^ψ, have inverse cascades. The presence of an inverse cascade process in conjunction with different dissipation rates (called selective decay) leads to self-organization, i.e., formation of large-scale coherent structures which are absent in Navier-Stokes turbulence. It is also noteworthy that in contrast to Navier-Stokes turbulence 2D and 3D MHD turbulence are rather closely related. The concept of spectral cascades implies that mode interactions are rather localized in k, i.e., modes with strongly different wave numbers interact only weakly. Though this appears to be true Navier-Stokes turbulence, there is a strong nonlocal process in MHD turbulence. While a large-scale velocity v_0 has no influence on the small-scale dynamics (it can be eliminated by a Galilean transformation) a large-scale magnetic field B_0 leads to strong coupling of small-scale velocity and magnetic field fluctuations. The effect can easily be demonstrated from Eqs. (4) and (5). Extracting $\mathbf{B}_0$ from $\mathbf{P}$ and $\mathbf{Q}$ we have

$$\partial_t \mathbf{P}-\mathbf{B}_0\cdot\nabla\mathbf{P}+\mathbf{Q}\cdot\nabla\mathbf{P}=-\nabla p_t+\nu_+\nabla^2\mathbf{P}+\nu_-\nabla^2\mathbf{Q}\ , \tag{9}$$

$$\partial_t \mathbf{Q}+\mathbf{B}_0\cdot\nabla\mathbf{Q}+\mathbf{P}\cdot\nabla\mathbf{Q}=-\nabla p_t+\nu_+\nabla^2\mathbf{Q}+\nu_-\nabla^2\mathbf{P}\ , \tag{10}$$

1063-651X/94/50(4)/2702(10)/$06.00

such that for $B_0 \gg P,Q$ the small-scale quantities **P** and **Q** behave as Alfvén waves, propagating oppositely to and in the direction of $\mathbf{B}_0$, respectively. This is called the Alfvén effect in MHD turbulence [2,3]. Since only oppositely propagating modes interact with the interaction time of two wave packets of scale l, $\tau_A = l/v_A$, $v_A = B_0$ in our units, the spectral energy transfer rate ϵ is reduced compared with the hydrodynamic case, which leads to the Iroshnikov-Kraichnan [2,3] inertial-range energy spectrum

$$E_k = C_{\mathrm{IK}}(\epsilon v_A)^{1/2} k^{-3/2}, \quad E_k^V \simeq E_k^M , \tag{11}$$

instead of the Kolmogorov spectrum

$$E_k = C_{\mathrm{Ko}} \epsilon^{2/3} k^{-5/3} , \tag{12}$$

where C_{Ko} and C_{IK} are (probably not universal) constants. Experiments and numerical simulations give $C_{\mathrm{Ko}} \sim 1.4$–2.2, while $C_{\mathrm{IK}} \sim 1.8$–2.2 [4]. Since laboratory experiments of MHD turbulence are difficult to perform, numerical modeling plays a particularly important role. To date direct numerical simulations for moderately high Reynolds numbers (R_λ a few hundred) have been limited to 2D systems, while 3D MHD turbulence simulations are still restricted to rather low Reynolds numbers. Because of the difficulties of solving the full fluid equations, simplified model systems, so-called shell or cascade models, have attracted considerable interest, primarily for Navier-Stokes turbulence [5–12] and thermal convection [13,14]. Cascade models involve three distinct approximation steps: (a) Integration over modes in shells Δk_n around wave numbers k_n thus averaging over the interactions between modes located in the same shell; (b) logarithmic spacing of $k_n, k_n = k_0 q^n, n = 1, \ldots, N$, corresponding to an increasing sparseness of the effective Fourier representation at larger k_n; usually $q=2$ is chosen; (c) local mode interactions in k_n space (not in k space, since Δk_n is finite), which corresponds to the picture of a cascade process in small steps. Though the vector character of the original quantities **v**,**B** could be incorporated in an approximate way, it is ignored for simplicity in most shell model studies which assume v_n, B_n to be (complex) scalars, hence the term scalar model also used in the literature. Shell models constitute an intermediate step between low-order approximations such as the Lorenz model and the full fluid equations, allowing statistical scaling properties but ignoring spatial coherence effects. Since such models only satisfy certain global conservation properties they exhibit substantial arbitrariness concerning both the structure of the nonlinear terms and the values of the coupling parameters. Hence the main interest in studies of such models is to reproduce qualitatively the main scaling properties known or expected for the fluid system and to investigate their dependence on the particular model chosen. Shell model computations for MHD turbulence have previously been performed by Gloaguen *et al.* [15]. Grappin, Léorat, and Pouquet [16], and Geertsema and Achterberg [17], and Brandenburg [14], all using essentially the model introduced in Ref. [15] with real functions v_n, B_n and ignoring the Alfvén effect. For the main part of this paper we use the same basic model, but generalized to complex variables which allow us to include the Alfvén effect in a simple way. Instead of v_n, B_n we use the Elsässer variables $P_n = v_n + B_n$, $Q_n = v_n - B_n$, following the equations

$$\begin{aligned} \dot{P}_n &= ik_n B_0 P_n + a(k_n P_{n-1}^* Q_{n-1}^* - k_{n+1} P_{n+1}^* Q_n^*) \\ &\quad + b(k_n P_{n-1}^* Q_n^* - k_{n+1} P_{n+1}^* Q_{n+1}^*) - k_n^{2\alpha} \nu_\alpha P_n + f_n , \\ \dot{Q}_n &= -ik_n B_0 Q_n + a(k_n Q_{n-1}^* P_{n-1}^* - k_{n+1} Q_{n+1}^* P_n^*) \\ &\quad + b(k_n Q_{n-1}^* P_n^* - k_{n+1} Q_{n+1}^* P_{n+1}^*) - k_n^{2\alpha} \nu_\alpha Q_n + g_n . \end{aligned} \tag{13}$$

Here a,b are arbitrary complex coupling constants. Since, however, a common factor can be pulled into the time normalization, only the ratio b/a is relevant. The first term on the right-hand side of Eqs. (13) represents the Alfvén effect and the dissipation terms are written for general order α of the dissipation operators ($\alpha=1$ corresponding to ordinary diffusion), but with the restriction to $\nu_- = 0$, i.e., unit magnetic Prandtl number $\nu/\eta = 1$. f_n, g_n are suitably chosen external forces applied in a certain n range to sustain a stationary state against dissipative decay. In the inviscid limit $\nu_\alpha = 0$ and with boundary conditions $P_0 = Q_0 = P_N = Q_N = 0$ these equations conserve the global quantities $E^+ = \frac{1}{4}\sum_n |P_n|^2$, $E^- = \frac{1}{4}\sum_n |Q_n|^2$, and hence the total energy $E = E^+ + E^-$ and the crosscorrelation $K = \frac{1}{2}(E^+ - E^-)$. No further quadratic invariant exists. To account also for the invariance of H or H^ψ a different model is constructed using second-order neighbor couplings introduced by Gledzer [7],

$$\begin{aligned} \dot{P}_n &= ik_n B_0 P_n + a[k_{n-1} P_{n-1}^* Q_{n-2}^* - k_{n-1} \alpha_q P_{n-2}^* Q_{n-1}^* - k_n P_{n+1}^* Q_{n-1}^* - k_n \beta_q P_{n-1}^* Q_{n+1}^* \\ &\quad + k_{n+1} \beta_q P_{n+1}^* Q_{n+2}^* + k_{n+1} \alpha_q P_{n+2}^* Q_{n+1}^*] - k_n^{2\alpha} \nu_\alpha P_n + f_n , \end{aligned} \tag{14}$$

$$\begin{aligned} \dot{Q}_n &= -ik_n B_0 Q_n + a[k_{n-1} Q_{n-1}^* P_{n-2}^* - k_{n-1} \alpha_q Q_{n-2}^* P_{n-1}^* - k_n Q_{n+1}^* P_{n-1}^* - k_n \beta_q Q_{n-1}^* P_{n+1}^* \\ &\quad + k_{n+1} \beta_q Q_{n+1}^* P_{n+2}^* + k_{n+1} \alpha_q Q_{n+2}^* P_{n+1}^*] - k_n^{2\alpha} \nu_\alpha Q_n + g_n , \end{aligned} \tag{15}$$

$$\alpha_q = \frac{q^m - 1 + q^{-m}}{q^m + 1 - q^{-m}}, \quad \beta_q = \frac{q^m - 1 - q^{-m}}{q^m + 1 - q^{-m}} ,$$

where $m=1$ leads to the (inviscid) conservation of $H=\sum_n |B_n|^2/k_n$, corresponding to the 3D case, while $m=2$ leads to conservation of $H^\psi=\sum_n |B_n|^2/k_n^2$, the quantity conserved in 2D. In addition both E^+ and E^-, i.e., E and K, are conserved. Hence the conservation laws uniquely determine the nonlinear terms, since the coupling constant a can again be incorporated in the normalization.

Neglecting the Alfvén effect and restricting to real P_n, Q_n Eqs. (13) have previously been investigated for relatively low orders, $N \leq 3$ in Ref. [15] and $N \lesssim 10$ in Refs. [16,17], with the emphasis on aspects of chaos theory such as attractor dimensions and Lyapunov exponents. While these concepts are very useful to describe the properties of low-order systems, they seem to be less relevant for $N \gg 1$, where the systems studied thus far (see, e.g., Ref. [10]) show attractor dimensions of the order of the number of degrees of freedom up to the dissipative scales and most of the Lyapunov exponents are very close to zero. Instead the tools of statistical turbulence theory are more appropriate, in particular probability density functions (PDF) and their moments, the structure functions.

Equations (13) and (14) are solved numerically using a modified Runge-Kutta *IV* scheme and $N=20-23$ modes. Combined with a higher-order dissipation operator $\alpha=2$ this gives an inertial range of 3–4 decades, which we find to be sufficient to determine the important scaling properties. Though the numerical advantage of cascade models compared with the full (i.e., nonsparse at high k) fluid equations is enormous, there is also a moderate price to be paid. While in a solution of the fluid equations spatial averages do not fluctuate strongly in time such that only relatively short time periods (~ 10 eddy turnover times) are required to obtain accurate statistical results, the "modes" in a cascade model fluctuate strongly (by several orders of magnitude), hence do not really behave as shell averages in spite of their formal construction, such that long periods (10^3-10^4 "eddy turnover times") are required. We choose the driving forces f_n, g_n such as to sustain the energies of the $n=n_0$ mode, typically $n_0=3$, usually with $|P_n|^2=|Q_n|^2$. Constant forces f_n, g_n, which were used in the previous cascade model studies, are found to lead to dynamical alignment with $E^+ \gg E^-$ or $E^+ \gg E^-$ even for $f_n=q_n$. Since in such states the dynamics is strongly reduced and scaling properties are less transparent, attention is focused in this paper on turbulence with $E^+ \simeq E^-$.

The organization of the paper is as follows. In Sec. II we discuss the stationary solutions and their stability. Sections III and IV are restricted to the case $B_0=0$. Section III deals with the special case $P_n=Q_n$, i.e., purely kinetic turbulence, while Sec. IV presents the general case, where P_n and Q_n are independent variables. In Sec. V the Alfvén effect $B_0 \neq 0$ is included and several models are discussed. Section VI deals with the properties of inverse cascades. In most of the paper consideration is restrictive to the Gloaguen model, Eqs. (13), the alternative model, Eqs. (14), is only briefly discussed in Sec. VI.

II. STATIONARY SOLUTIONS

We are primarily interested in similarity or scaling solutions

$$P_n \sim k_n^\kappa, \quad Q_n \sim k_n^\lambda , \tag{16}$$

which can be strictly valid only in the limit $\nu_\alpha \to 0$. Insertion into Eqs. (13) gives

$$q^{-\kappa-\lambda} - q^{1+\lambda} + \frac{b}{a}(q^{-\lambda} - q^{1+\kappa+\lambda}) = 0 ,$$

$$q^{-\kappa-\lambda} - q^{1+\kappa} + \frac{b}{a}(q^{-\kappa} - q^{1+\kappa+\lambda}) = 0 ,$$

or

$$(1-q^{1+\kappa+2\lambda})\left[1+\frac{b}{a}q^\kappa\right]=0 ,$$
$$(1-q^{1+2\kappa+\lambda})\left[1+\frac{b}{a}q^\lambda\right]=0 . \tag{17}$$

Kolmogorov-type solutions

$$\kappa=\lambda=-\tfrac{1}{3} \tag{18}$$

exist for any value of b/a. Further simple scaling solutions of (17) require real $b/a<0$, either

$$\kappa=\lambda=-\log_q\left|\frac{b}{a}\right| , \tag{19}$$

or

$$\kappa=-\log_q\left|\frac{b}{a}\right|, \quad \lambda=-(1+2\kappa) , \tag{20}$$

or vice versa. For $b/a>0$ there are somewhat more general scaling solutions, alternating in phase between successive values of n,

$$P_n \sim Q_n \sim k^\kappa \cos n\pi ,$$
$$\kappa=-\log_q\frac{b}{a} , \tag{21}$$

while no solution with $\kappa \neq \lambda$ analogous to Eq. (20) exists for $b/a>0$. For special values of a and b we can also give nonscaling stationary solutions, in particular for $b=0$,

$$P_n \sim Q_n \sim k_n^{-1/3}\exp\{C(-2)^n\} , \tag{22}$$

i.e., with increasing n the amplitude diverges exponentially from the $k_n^{-1/3}$ behavior, or for $a=0$

$$P_n \sim Q_n \sim k_n^{-1/3}\exp\{C(-2)^{-2n}\} , \tag{23}$$

i.e., exponential convergence to the $k_n^{-1/3}$ behavior. In the expressions (22), (23) C is an arbitrary complex number. In the special case $C=i$, the amplitudes follow the Kolmogorov law, but the phases in Eq. (22) become effectively random for large n.

For the stationary solutions to be physically relevant (in the inertial range) one has to investigate their stability. Desnyanski and Novikov [6] study the stationary deviations φ_n from the Kolmogorov solution by introducing dissipation localized at $n \geq N$, writing

$$P_n = P_0 k_n^{-\frac{1}{3}+\varphi_n} \propto Q_n . \tag{24}$$

Linearization of Eqs. (13) with respect to the stationary perturbation φ_n gives

$$2\varphi_{n-1}+\varphi_n-(\varphi_{n+1}+\varphi_n)+\frac{b}{aq^{1/3}}(\varphi_{n-1}-2\varphi_{n+1})=0 ,$$

which yields the recursion relation for $\delta\varphi_n=\varphi_{n+1}-\varphi_n$:

$$\delta\varphi_{n-l}=(-A)^l\delta\varphi_n ,$$
$$A=\left[2\frac{b}{aq^{1/3}}+1\right]\Big/\left[\frac{b}{aq^{1/3}}+2\right] . \tag{25}$$

For $|A|>1$ the perturbation is exponentially growing from its origin in the dissipation region into the inertial region while for $|A|<1$, the Kolmogorov solution remains effectively unaffected by the presence of the dissipation. This behavior for large and small $|b/a|$ is reminiscent of the solutions (22) and (23) for $a=0$ and $b=0$, respectively.

Let us briefly consider the solution in the dissipation region in more detail. Writing $P_n=k_n^{-1/3}p_n$, $Q_n=k_n^{-1/3}q_n$, following the analysis by Bell and Nelkin [8] we find to lowest order

$$aq^{2/3}p_{n-1}q_{n-1}-\nu k_n^{4/3}p_n\simeq 0 ,$$
$$aq^{2/3}p_{n-1}q_{n-1}-\nu k_n^{4/3}q_n\simeq 0 ,$$

which gives

$$p_n\simeq q_n\propto k_n^{4/3}\exp\left[-Ck_n\left[\frac{2}{q}\right]^n\right] . \tag{26}$$

Hence only for $q=2$ the exponential behavior in the dissipation observed in all fluid turbulence systems is recovered in the cascade model, which indicates a special significance of this value. For this reason and following convention we henceforth restrict consideration to $q=2$. Numerical solution of the time dependent equations (13) for real values a,b and real initial conditions $P_n=Q_n$ (kinetic case $B_n=0$) shows that the system is always attracted to a stationary state, the Kolmogorov solution (18) in the stable range $|b/a|<2^{1/3}$, the "unstable" Kolmogorov solution similar to Eq. (22) for $b/a>2^{1/3}$, and the non-Kolmogorov solution (19) for $b/a<-2^{1/3}$. A somewhat different situation arises for real initial values $P_n=-Q_n$ (magnetic case $v_n=0$). Here we find "aligned" structures $|P_n|\gg|Q_n|$ or vice versa for $|b/a|<2^{1/3}$, somewhat reminiscent of the stationary solution (20), while solution (19) is valid for $b/a<-2^{1/3}$ and solution (21) for $b/a>2^{1/3}$.

In the case of the stationary Kolmogorov solution the energy dissipation rate ϵ is independent of the dissipation coefficients. We can easily calculate ϵ and the Kolmogorov constant C in this case. Writing $P_n=Q_n=u_n$, using the definition of the energy transfer rate

$$\epsilon=\epsilon^+ +\epsilon^-$$
$$=2\sum_{n=1}^{N}u_n[a(k_nu_{n-1}^2-k_{n+1}u_nu_{n+1})$$
$$+b(k_nu_nu_{n-1}-k_{n+1}u_{n+1}^2)-\nu k_n^2u_n] , \tag{27}$$

and concentrating dissipation in the last shell such that $u_n=u_0k_n^{-1/3}$ for $n<N$ and $u_N=0$, we obtain

$$\epsilon=2u_0^3(2^{2/3}a+2^{1/3}b) . \tag{28}$$

From the energy spectrum

$$E=u_0^2k_n^{-5/3}=C\epsilon^{2/3}k_n^{-5/3}$$

we find

$$C=(2^{4/3}a+2b)^{-2/3} .$$

These analytical results agree with the numerically obtained solution. Note that both ϵ and C depend on the magnitude of the coupling constants. Since there is no preferred normalization, such as $a=1$ or $b=1$, the cascade model does not predict a definite value of C. The stability limit $b/a=2^{1/3}$ can be associated with the behavior of the space volume $d\tau=\prod_{n=1}^{N-1}du_n$,

$$d\dot{\tau}=\sum_{n=1}^{N-1}\frac{\partial\dot{u}_n}{\partial u_n}d\tau \tag{29}$$
$$=-\sum_{n=1}^{N-1}(ak_{n+1}u_{n+1}-bk_nu_{n-1})d\tau , \tag{30}$$

hence $d\dot{\tau}\lesssim 0$ for $b/a\lesssim 2^{1/3}$ assuming $u_n=k_n^{-1/3}$. Note that in the case of real $P_n=Q_n$ Liouville's theorem $d\dot{\tau}=0$ is not valid. It is, however, valid for complex P_n,Q_n even for $P_n=Q_n$, since $\mathrm{Re}P_n$ and $\mathrm{Im}P_n$ are independent variables. Allowing general complex initial conditions results in fully turbulent states with spectra close to the Kolmogorov one. Only in a certain range around the stability points $|b/a|=2^{1/3}$ is the system attracted to periodic or weakly turbulent states resembling the stationary solution (19) (for $b/a\lesssim -2^{1/3}$) and (21) (for $b/a\gtrsim 2^{1/3}$).

III. TURBULENT KINETIC STATES

Before treating the general turbulent case (Secs. IV and V) we discuss the purely kinetic (complex) case $P_n=Q_n$. For identical forces $f_n=g_n$ the symmetry of the equations guarantees that $P_n=Q_n$ for all times if so initially. Let us first consider the case of about equal coupling constants $a\sim b$. Though for $P_n=Q_n$ Eqs. (13) become a shell model approximation of the Navier-Stokes equation, the statistical properties are quite different from those observed in Navier-Stokes turbulence. While the time traces of $\mathrm{Re}P_n$ and $\mathrm{Im}P_n$ exhibit a strongly turbulent behavior with zero mean value, PDF's reveal that the system also contains a laminar contribution. Figure 1 gives $f(\mathrm{Im}P_n)$ for $n=8,14$, both in the inertial range, of a case with $a=b=i$. This δ-function-like laminar contribution at $P_n=P_n^l$ shows a Kolmogorov scaling law $P_n^l\sim k_n^{-1/3}$. The total energy spectrum, however, is steeper, $E_n\sim k_n^{-\alpha}$, $\alpha=1.74\pm 0.01$, as shown in Fig. 2. Hence with increasing n the laminar contribution moves further out into the wings of the PDF, as seen in Fig. 1. We thus find that the system though fully turbulent still remembers the corresponding stationary solution (18). In contrast to fluid turbulence, where coherent structures are observed in space, the P_n^l states which occur in this shell model approximation can be considered as coherent

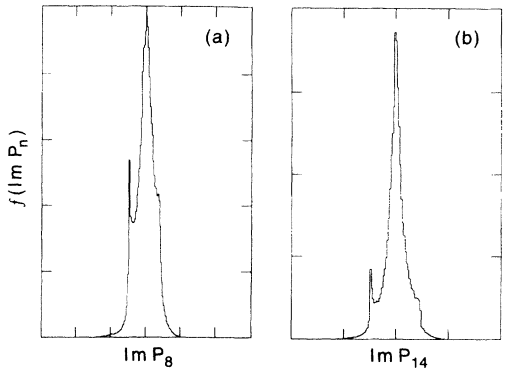

FIG. 1. PDF of $\mathrm{Im}P_n$ for $a=b=i$ plotted on a linear scale. (a) $n=8$, (b) $n=14$.

structures in k space. While for imaginary coupling coefficients the coherent contribution is essentially imaginary $|\mathrm{Im}P_n^I| \gg |\mathrm{Re}P_n^I|$, it is essentially real $|\mathrm{Re}P_n^I| \gg |\mathrm{Im}P_n^I|$ for almost real a,b. (In the case of strictly real a,b the solution relaxes to a stationary state.)

Coherent turbulent states are restricted to the coupling range $a \sim b$, whereas for $|b| \gg |a|$ the coherent component vanishes and the turbulence spectrum is close to Kolmogorov. This confirms the argument by Gloaguen *et al.* [15] that the case $a \ll b$ is more representative of incompressible turbulence, since the a term refers to wave number triads corresponding to flat triangles which have negligible weight in the nonlinear interactions. The triangle condition of interacting wave number triads is, however, less stringent than suggested by the discussion in Ref. [15], since shell modes P_n represent all physical modes located in the shell $2^n/\sqrt{2} < k < 2^n < \sqrt{2}$. [When applying the strict argument of Ref. [15] all interactions in Gledzer-type models such as Eqs. (14) would be forbidden.] But the available k-space volumes of a-type interactions are smaller than those of b-type interactions. Calculation of these volumes, which depend on the spatial dimension, would give an estimate of b/a representative of fluid turbulence.

IV. FULLY DEVELOPED MHD TURBULENCE NEGLECTING THE ALFVÉN EFFECT

We now consider the general case of complex P_n, Q_n with $P_n(t) \neq Q_n(t)$, which for most values b/a of the coupling constants leads to fully developed MHD turbulence. Turbulent states with a Kolmogorov spectrum $E_n \sim k_n^{-\alpha}$, $\alpha = 1.66 \pm 0.02$ are found for $b/a < 1$, with the exception of a small region around $b/a \simeq -2^{1/3}$. In the range $1 \lesssim b/a < 2^{1/3}$ one finds turbulent states with a somewhat steeper spectrum $\alpha \simeq 1.75$. For $b/a \simeq 2^{1/3}$ there is transition to the stationary solution (21), which is stable in the range $2^{1/3} \simeq b/a \simeq 3$, while for $b/a > 3$ we find again turbulent states with a Kolmogorov spectrum. Hence the stationary solutions (19) and (20) are completely wiped out, while only the stationary solution (21) is stable with respect to general complex perturbations in the range indicated. The boundaries between the different types of solution are rather soft, depending on the initial conditions and the way of external forcing.

It is worth mentioning that the energy spectra do not assume an exact power law but exhibit (stationary) oscillations about a mean power law. These are not due to insufficient statistical sampling but persist in the limit $t \to \infty$. While the oscillation amplitude is in general small, they become quite substantial for certain values of b/a. An extreme example is obtained for $b=0$ (Fig. 3) which nevertheless corresponds to a state of fully developed turbulence. The spectrum is well converged numerically, and the oscillations in the "inertial" range are invariant to a change of the dissipation coefficient. In general stronger oscillatory deviations from a pure power-law behavior occur in the higher-order structure

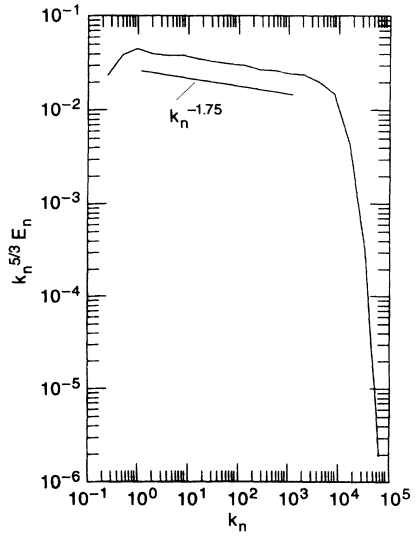

FIG. 2. Compensated energy spectrum $k_n^{5/3}E_n$ for the case of Fig. 1.

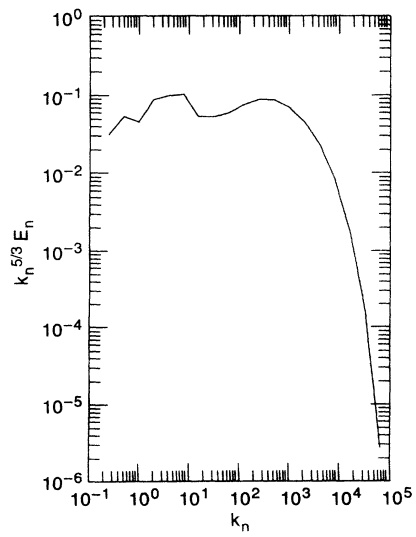

FIG. 3. Compensated energy spectrum $k_n^{5/3}E_n$ for $b=0$, exhibiting oscillations around a pure power law.

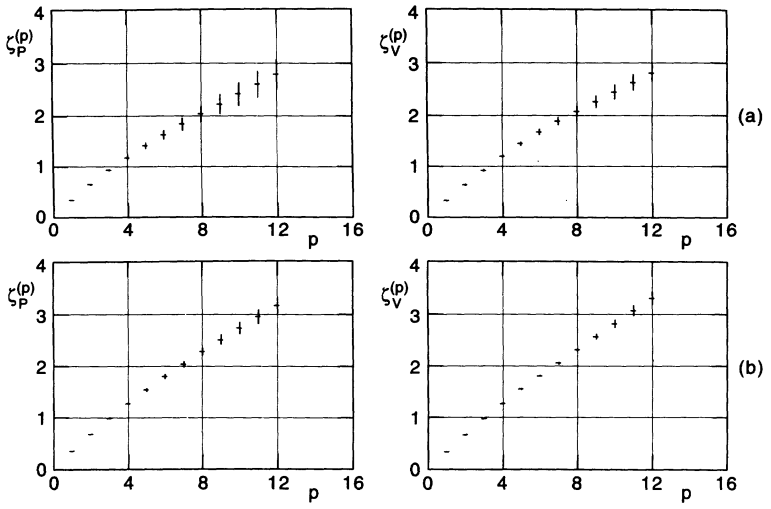

FIG. 4. Structure exponents $\zeta_P^{(p)}$ and $\zeta_V^{(p)}$ for (a) $b/a=-0.75$, (b) $b/a=10^2$.

functions discussed below. This behavior, which has also been observed in fluid turbulence [18], can be associated with the lacunarity of the fractal attractor of the turbulence [19]. It is also interesting to consider the kinetic and magnetic energy spectra $E_n^V=\frac{1}{4}|P_n+Q_n|^2/k_n$, $E_n^M=\frac{1}{4}|P_n-Q_n|^2/k_n$. Though we find that E_n^M is consistently slightly steeper than E_n^V, $E_n^M/E_n^V\sim k^{-0.04}$, the normalized reduced spectrum $(E_n^M-E_n^V)/E_n$ is much smaller and more steeply decreasing with n than observed in MHD fluid turbulence [4]. This behavior is rather unexpected, since the Alfvén effect, which in fluid turbulence is invoked to lead to a strong coupling of v_k and B_k and hence a small value of the normalized reduced spectrum, is at this point not accounted for in our cascade model calculations. A simple explanation of the equality of E_n^M and E_n^V is given by the observation that P_n and Q_n are practically statistically independent, $E_n^V=|P_n+Q_n|^2\simeq|P_n|^2+|Q_n|^2\simeq E_n^M$.

The statistical properties of a turbulent fluid are conveniently described by the PDF's of the velocity increments $\delta v_l=v(x+l)-v(x)$, or equivalently the moments thereof called the structure functions $f^{(p)}=\langle\delta v_l^p\rangle$. In a cascade model, where real space quantities such as δv_l are not defined, one considers instead PDF's and moments of the Fourier components, the shell quantities such as v_n, which are related to δv_l with $l=k_n^{-1}$. We consider the quantities $\mathrm{Re}P_n$, $\mathrm{Re}Q_n$, $\mathrm{Re}v_n=\frac{1}{2}\mathrm{Re}(P_n+Q_n)$, $\mathrm{Re}B_n=\frac{1}{2}\mathrm{Re}(P_n-Q_n)$. The corresponding functions are denoted by $f_P^{(p)}(n)$, $f_Q^{(p)}(n)$, $f_V^{(p)}(n)$, $f_B^{(p)}(n)$. We also evaluate the normalized structure functions $F^{(p)}(n)=f^{(p)}(n)/[f^{(2)}(n)]^{p/2}$, which illustrate deviations from Gaussian statistics particularly clearly. In the inertial range the structure functions follows closely (apart from the lacunarity oscillations discussed above) a power law $f^{(p)}(n)\sim k_n^{\zeta(p)}$. In general the values of the structure exponents $\zeta_P(p)$, $\zeta_Q(p)$, $\zeta_V(p)$, $\zeta_B(p)$ are found to be equal within the error bars. They do, however, depend on the coupling coefficients. Figure 4 gives $\zeta_P(p)$ and $\zeta_V(p)$ for $b/a=-0.75$ and $b/a=10^2$. The error bars obtained from a least-squares fit of the structure function to a power law in the interval $n_0+1\le n\le 14$ are primarily due to lacunarity oscillations. In both cases energy spectra are consistent with $k_n^{-5/3}$, i.e., $\zeta(2)\simeq\frac{2}{3}$, but higher-order structure exponents differ significantly in the two cases. The deviation from the Kolmogorov scaling $\zeta(p)=p/3$ is a measure of (temporal) intermittency, and the deviation from a linear behavior is associated with a multifractal structure of the turbulent attractor [21]. Hence we find that $b/a\sim 1$ gives rise to a stronger multifractal behavior than $b/a\gg 1$. The values of $\zeta(p)$ in the latter case are close to those obtained from the Gledzer-Ohkitani-Yamada model for hydrodynamic turbulence [12], which agree with the experimental observations [18] and 3D fluid simulation [20]. This again confirms the argument by Gloaguen *et al.* [15].

Figure 5 gives the normalized structure functions $F^{(4)}$ and $F^{(6)}$ of the variable $\mathrm{Re}P_n$ for the case $b/a=-0.75$. While for $n\sim 1$ the statistics are close to Gaussian, $F^{(4)}\simeq 3$, $F^{(6)}\simeq 15$, it is increasingly non-Gaussian for high

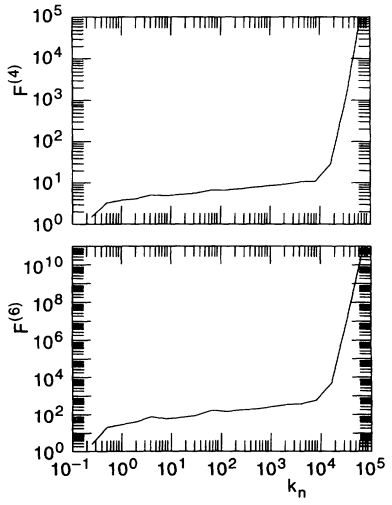

FIG. 5. Normalized structure function $F^{(4)}$,$F^{(6)}$ of $\mathrm{Re}P_n$ for $b/a=-0.75$.

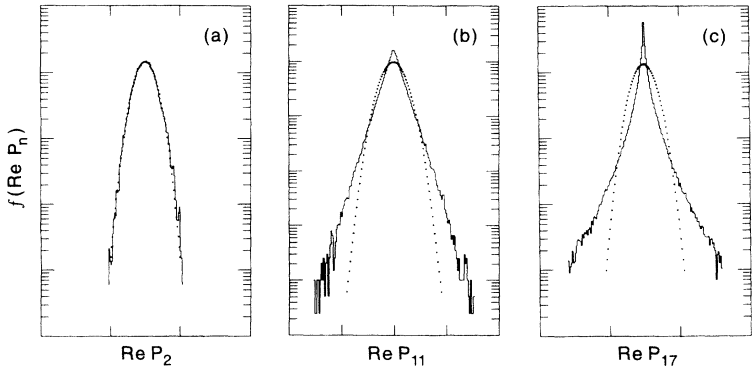

FIG. 6. PDF's of $\mathrm{Re}P_n$ for the same case as in Fig. 5 for $n=2,11,17$.

n in the inertial range and shows a much stronger increase in the dissipation range $n \gtrsim 16$.

Figure 6 illustrates the increasingly non-Gaussian behavior of the PDF's. At the highest mode number given, $n=17$, which belongs to the dissipation range, the PDF has a δ-function contribution at zero argument which originates from the stiff oscillations of the dissipation range spectrum according to the fluctuation of the energy dissipation rate ϵ. It is interesting to note that the latter exhibits an almost precise log-normal distribution (Fig. 7).

V. MODELS OF THE ALFVÉN EFFECT

Let us now consider the influence of the Alfvén effect, the first term on the right-hand side of Eqs. (13). From the way this effect is usually discussed we expect that choosing a constant B_0 will change the energy spectrum from Kolmogorov to $k^{-3/2}$. However, as we will see, this is not what is found numerically; the Alfvén effect appears to be more subtle. We note that the addition of the B_0 term formally destroys the scale invariance of the (nondissipative) equations (13) by introducing the Alfvén time $(k_n B_0)^{-1}$. Hence there can be no universal power-law spectrum over the entire k range. Using simple scaling arguments we expect a crossover from a $k^{-5/3}$ to a $k^{-3/2}$ spectrum at the point k_c, where the Alfvén time $(kB_0)^{-1}$ equals the eddy turnover time which is obtained by equating both spectra,

$$\epsilon^{2/3}k^{-5/3}=(\epsilon B_0)^{1/2}k^{-3/2} ,$$

which gives

$$k_c=\epsilon/B_0^3 . \tag{31}$$

This crossover is in fact observed numerically. Figure 8 gives the energy spectra for three cases with different values of B_0 with $k_c \simeq 600,25,1$ for $B_0=0.1,0.3,1$, respectively, which is consistent with the scaling (31). The spectral laws for $k<k_c$ and $k>k_c$ differ, however, from the expected power laws $k^{-5/3}$ and $k^{-3/2}$, respectively, being steeper in the first case, $\sim k^{-1.7}$, and shallower in the latter, $\sim k^{-\alpha}$, $\alpha=1.25-1.3$. For $B_0=1$ the $k^{-1.25}$ spectral law extends over the entire inertial range. Hence the constant B_0 model of the Alfvén effect does not

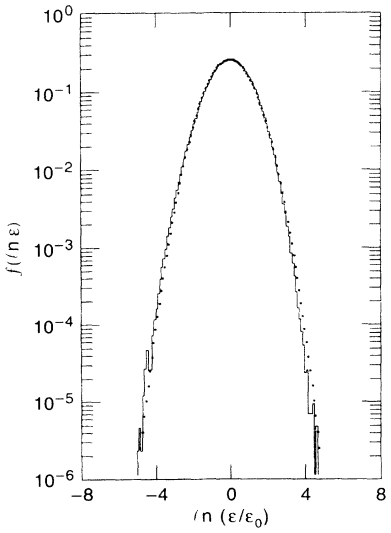

FIG. 7. PDF of $\ln\epsilon$ for the same case as in Fig. 5.

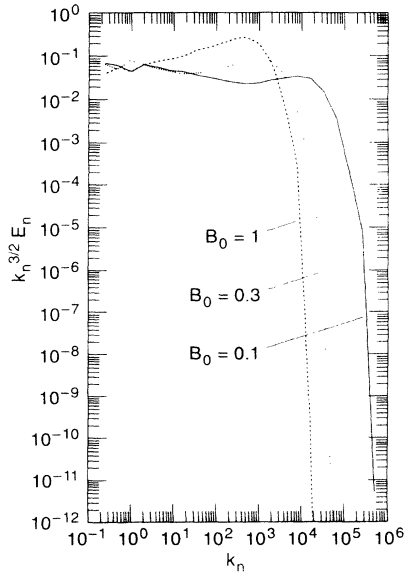

FIG. 8. Compensated energy spectra $k_n^{3/2}E_n$ for $b/a=10^2$ and different values of $B_0=$const.

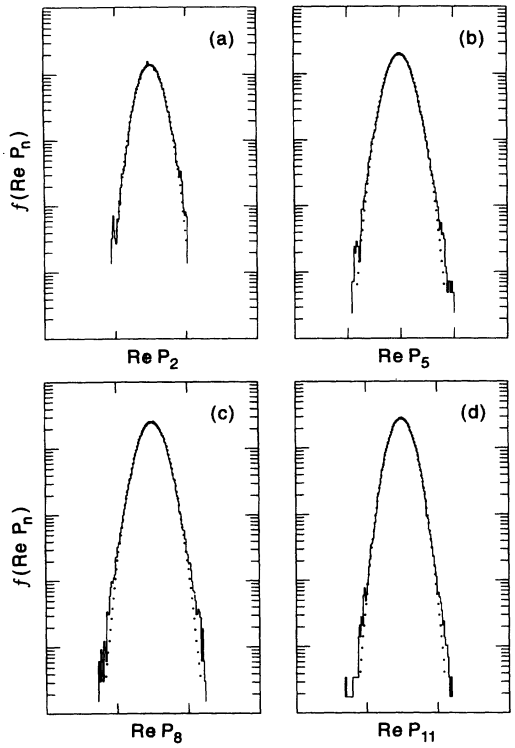

FIG. 9. PDF of $\mathrm{Re}P_n$ for case $B_0=1$, of Fig. 8 for $n=2,5,8,11$.

reproduce the Iroshnikov-Kraichnan spectrum, which has been observed in high resolution simulation of 2D MHD turbulence [4,22]. An even more significant discrepancy arises in the statistical properties. We find that in the B_0-dominated part of the spectrum $k>k_c$ statistics are strictly Gaussian (Fig. 9) down to the dissipation range, where strong non-Gaussian behavior is generated by the fluctuations of ϵ. By contrast, numerical simulations of 2D MHD turbulence [22] show a distinct non-Gaussian behavior in the inertial range, similar to that in 3D hydrodynamic turbulence [20]. It is interesting to relate our results to the behavior observed in computations of the Fourier-Weierstrass model [23] which can be regarded as a sophisticated shell model including multilevel interactions. As in the case of the constant-B_0 Alfvén effect the Fourier-Weierstrass model does not exhibit inertial-range intermittency. A possible reason for this unphysical feature could be a relative overestimate of the nonlocal interactions. Instead of considering B_0 a constant external parameter it should be the actually present magnetic field of the large-scale turbulent eddies. Hence we choose P_n, Q_n,

$$B_0(t)=B_0^{(n)}(t)=\alpha\sum_{j=2}^{n-1}\mathrm{Re}(P_j-Q_j)\ . \tag{32}$$

In this case B_0 has a Gaussian distribution. This implies that for large-scale modes the Alfvén effect is only occasionally active when B_0 happens to be sufficiently large, while small-scale modes are practically always magnet-

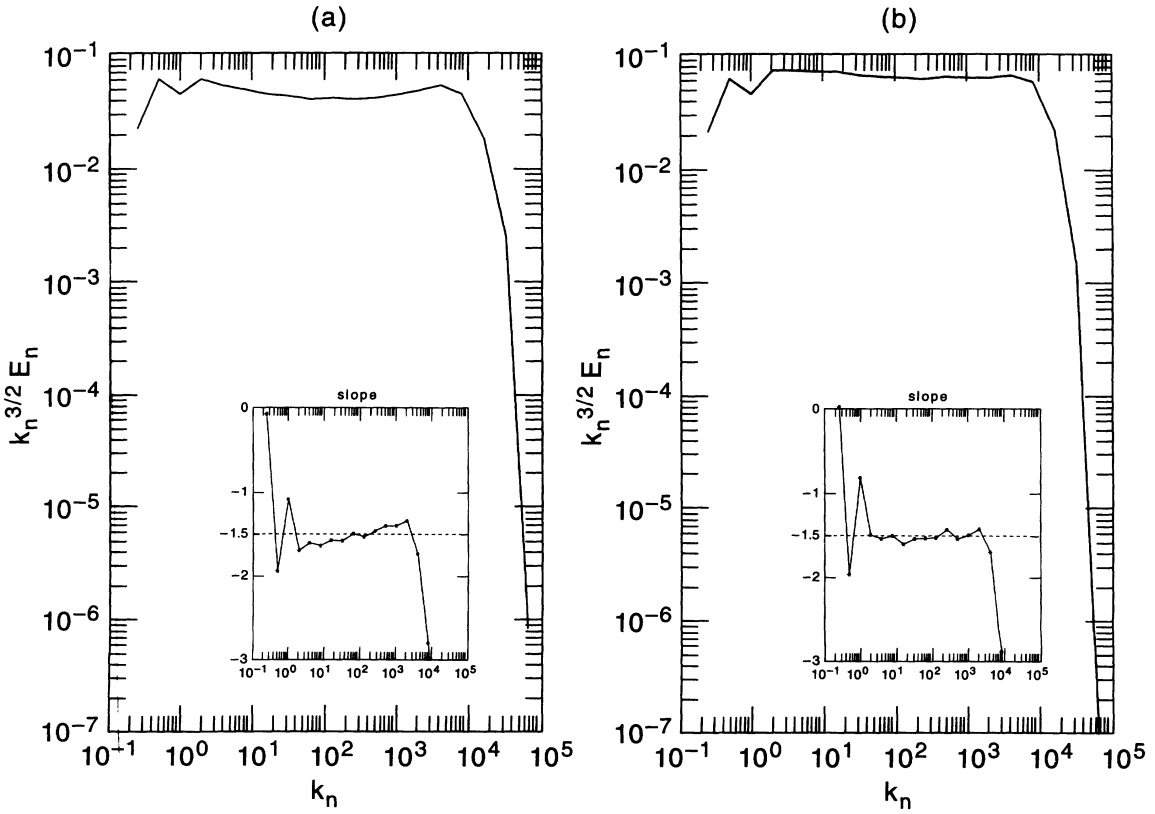

FIG. 10. Compensated energy spectra $k_n^{3/2}E_n$ for $a/b=10^2$ using the model (32), $\alpha=0.5$ and 2.

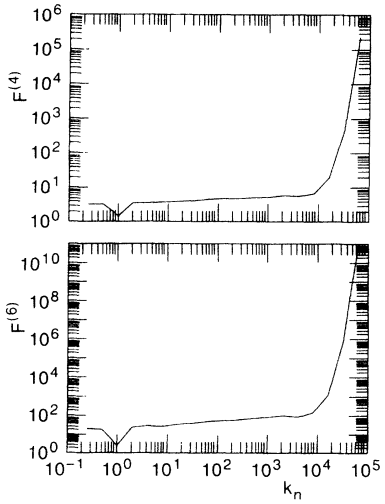

FIG. 11. Normalized structure functions $F^{(4)},F^{(6)}$ for $b/a=10^2$ and the Alfvén effect model (32) with $\alpha=2$.

ized. The coefficient α is an adjustable parameter of order unity. Figure 10 gives the energy spectra of two cases for $b/a=10^2$, with $\alpha=0.5$ and 2. The spectrum for $\alpha=0.5$ is reminiscent of those shown in Fig. 8 for constant B_0. However, instead of a rather sharp crossover at $k_n=k_c$ between two well-defined scaling ranges the transition is gradual. For $\alpha=2$ the energy spectrum agrees with a $k^{-3/2}$ law. The statistical properties are clearly nonGaussian, which is different from the nonintermittent behavior of the $B_0=$const case. Figure 11 gives the normalized structure functions $F^{(4)},F^{(6)}$, which show the linear increase with k_n in the inertial range, which is, however, somewhat weaker than in the nonmagnetic case, Fig. 5. This is in qualitative agreement with the influence of the Alfvén effect in the β model [24].

VI. INVERSE CASCADES

As mentioned in the Introduction, MHD turbulence is characterized by the coexistence of direct and inverse cascade processes. If the system is driven at large scales the former dominates, if it is driven at small scales the latter dominates, generating increasingly larger scales. Simple scaling arguments predict [1] the inverse cascade spectrum of the magnetic helicity

$$H_k \propto k^{-2} \tag{33}$$

and in 2D the mean square potential spectrum

$$H_k^{\psi} \propto k^{-7/3} . \tag{34}$$

The latter has recently been verified in numerical simulations of driven 2D MHD turbulence [25]. The most significant deficiency of cascade models seems to be their inability to reproduce the inverse cascade properties. The spectrum is found to be $E_n \sim k_n^{-1}$, i.e., $H_n^{\psi} \sim k_n^{-3}$, which corresponds to equipartition of mode amplitudes $\langle |P_n| \rangle \simeq \langle |Q_n| \rangle \simeq$const. The system is fully turbulent, since $|P_n|=$const is not a stationary solution. There is also no condensation in the lowest k mode $n=1$, independent of the boundary condition at $n=0$ (both $P_0=0$ and $P_0=P_1$ give the same behavior). The result is also independent of the other relevant parameters such as b/a or the modeling of the Alfvén effect (which by the way is negligible in the inverse cascade of H_k^{ψ}, see Ref. [25]), and also of the particular choice of the cascade model. Equations (14) are constructed to conserve explicitly a second global quantity such as H^{ψ}, but nevertheless lead to the equipartition spectrum $E_n \sim k_n^{-1}$.

It is interesting to note that the statistics in the "inverse cascade" region $n<n_0$ are exactly Gaussian, while remaining non-Gaussian in the region $n>n_0$. Such behavior is also observed in fluid simulations of inverse cascade processes [25,26], which are, however, driven in a random way. In our cascade model calculations the driving is coherent, either by constant forces or by imposing constant amplitudes. It thus appears that Gaussian statistics are a generally valid property of inversely cascading turbulence, even in model systems that do not reproduce the spectral properties of the corresponding fluid systems.

VII. CONCLUSIONS

We have presented studies of cascade models for MHD turbulence. Most of the computations are performed using the complex version of the model introduced by Gloaguen *et al.* [15], but we have also derived an alternative model which conserves the equivalent of the magnetic helicity (or the mean square potential in 2D). In the first part of the paper the Alfvén effect has been neglected. We discuss the stationary solutions, most of which are unstable, and the system evolves into a fully turbulent state. For purely kinetic turbulence $P_n=Q_n$ a phenomenon called coherent structures in k_n space is presented. It consists of a laminar component with the scaling $k_n^{-5/3}$ superimposed on a steeper turbulent spectrum $k_n^{-1.75}$, both being tightly interwoven, becoming visible only in the PDF's. In the general magnetohydrodynamic case (still in the absence of the Alfvén effect) fully developed turbulence with a Kolmogorov spectrum is found. The inertial-range statistics, in particular the structure functions, are similar to those observed in hydrodynamic (fluid) turbulence, depending quantitatively on the ratio of the coupling parameters, a,b, with the best agreement reached for $a \ll b$. In the second part of the paper the Alfvén effect is included. For the simplest case of a constant large-scale field B_0 energy spectra are flatter, $E_n \sim k_n^{-1.25}$, than the expected Iroshnikov-Kraichnan law $k_n^{-3/2}$. More importantly the inertial-range statistics are exactly Gaussian, in contrast to full fluid MHD simulations. Hence the simple model is not valid and has to be confined. Assuming B_0 to be the actual fluctuating field, intermittency is reintroduced and the spectrum is close to $k_n^{-3/2}$ though it tends to be flatter for high k_n, such that there may not be a uniformly valid inertial-range power-law spectrum.

ACKNOWLEDGMENT

The author wishes to express his thanks to Elisabeth Schwarz for her assistance in the numerical computations.

[1] See, e.g., D. Biskamp, *Nonlinear Magnetohydrodynamics* (Cambridge, Cambridge, England, 1993), Chap. 7.
[2] P. S. Iroshnikov, Astron. Zh. **40**, 742 (1963) [Sov. Astron. **7**, 566 (1964)].
[3] R. H. Kraichnan, Phys. Fluids **8**, 1385 (1965).
[4] D. Biskamp and H. Welter, Phys. Fluids B **1**, 1964 (1989).
[5] A. M. Obukhov, Atmos. Oceanic Phys. **7**, 41 (1971).
[6] V. N. Desnyanski and E. A. Novikov, Prik. Mat. Mekh. **38**, 507 (1974) [J. Appl. Math. Mech. **38**, 468 (1974)].
[7] E. B. Gledzer, Dokl. Akad. Nauk SSSR **208**, 1046 (1973) [Sov. Phys. Dokl. **18**, 216 (1973)].
[8] T. L. Bell and M. Nelkin, Phys. Fluids **20**, 345 (1977).
[9] R. M. Kerr and E. D. Siggia, J. Stat. Phys. **19**, 543 (1978).
[10] M. Yamada and K. Ohkitani, J. Phys. Soc. Jpn. **56**, 4210 (1987); Prog. Theor. Phys. **79**, 1265 (1988); Phys. Rev. Lett. **60**, 983 (1988).
[11] M. H. Jensen, G. Paladin, and A. Vulpiani, Phys. Rev. A **43**, 798 (1991).
[12] D. Pisarenko, L. Biterale, D. Courvoisier, U. Frisch, and M. Vergassola, Phys. Fluids. A **5**, 2533 (1993).
[13] M. H. Jensen, G. Paladin, and A. Vulpiani, Phys. Rev. A **45**, 7214 (1992).
[14] A. Brandenburg, Phys. Rev. Lett. **69**, 605 (1992).
[15] C. Gloaguen, J. Léorat, A. Pouquet, and R. Grappin, Physica D **17**, 154 (1985).
[16] R. Gappin, J. Léorat, and A. Pouquet, J. Phys. (Paris) **47**, 1127 (1986).
[17] G. Geertsema and A. Achterberg, Comput. Phys. Commun. **59**, 154 (1985).
[18] F. Anselmet, Y. Gagne, E. Hopfinger, and R. Antonia, J. Fluid Mech. **140**, 163 (1984).
[19] L. A. Smith, J. D. Fournier, and E. A. Spiegel, Phys. Lett. **114A**, 465 (1986).
[20] A. Vincent and M. Meneguzzi, J. Fluid Mech. **225**, 1 (1991).
[21] See, e.g., G. Paladin and A. Vulpiani, Phys. Rep. **156**, 147 (1987).
[22] D. Biskamp, Chaos, Solitons Fractals (to be published).
[23] See, e.g., J. Eggers and S. Grossmann, Phys. Fluids A **3**, 1958 (1991).
[24] See, e.g., Ref. [1], p. 228.
[25] D. Biskamp and U. Bremer, Phys. Rev. Lett. **72**, 3819 (1994).
[26] L. M. Smith and V. Yahkot, Phys. Rev. Lett. **71**, 352 (1993).